

# Two robust nonconforming $H^2$ -elements for linear strain gradient elasticity

Hongliang Li<sup>1</sup> · Pingbing Ming<sup>2,3</sup> ·  
Zhong-ci Shi<sup>2,3</sup>

Received: 20 January 2016 / Revised: 6 January 2017  
© Springer-Verlag Berlin Heidelberg 2017

**Abstract** We propose two finite elements to approximate a boundary value problem arising from strain gradient elasticity, which is a high order perturbation of the linearized elastic system. Our elements are  $H^2$ -nonconforming while  $H^1$ -conforming. We show both elements converge in the energy norm uniformly with respect to the perturbation parameter.

**Mathematics Subject Classification** Primary 65N30 · 65N15; Secondary 74K20

## 1 Introduction

Strain gradient theory, which introduces the high order strain and microscopic parameter into the strain energy density, is one of the most successful approach to characterize the strong size effect of the heterogeneous materials [20]. The origin of this theory can be traced back to Cosserat brothers' celebrated work [13]. Further development

---

✉ Pingbing Ming  
mpb@lsec.cc.ac.cn

Hongliang Li  
lihongliang@mtrc.ac.cn

Zhong-ci Shi  
shi@lsec.cc.ac.cn

<sup>1</sup> Institute of Electronic Engineering, China Academy of Engineering Physics, Mianyang 621900, China

<sup>2</sup> The State Key Laboratory of Scientific and Engineering Computing, Academy of Mathematics and Systems Science, Chinese Academy of Sciences, No. 55, Zhong-Guan-Cun East Road, Beijing 100190, China

<sup>3</sup> University of Chinese Academy of Sciences, Beijing 100049, China

is related to Mindlin's work on microstructure in linear elasticity [23,24]. However, Mindlin's theory is less attractive in practice because it contains too many parameters. Based on Mindlin's work, Aifantis et al. [3,28] proposed a linear strain gradient elastic model with only one microscopic parameter. This simplified strain gradient theory successfully eliminated the strain singularity of the brittle crack tip field [14].

The strain gradient elastic model of Aifantis' is a perturbed elliptic system of fourth order from the view point of mathematics. To discretize this model by a finite element method, a natural choice is  $C^1$  finite elements such as Argyris triangle [5] and Bell's triangle [7] because this model contains the gradient of strain. We refer to [2,27,32,33] for works in this direction. Alternative approach such as mixed finite element has been employed to solve this model [4]. A drawback of both the conforming finite element method and mixed finite element method is that the number of the degrees of freedom is extremely large and high order polynomial has to be used in the basis function, which is more pronounced for three dimensional problems; See e.g., the finite element for three-dimensional strain gradient model proposed in [27] contains 192 degrees of freedom for the local finite element space.

A common approach to avoid such difficult is to use the nonconforming finite element. For scalar version of such problem, there are a lot of work since the original contribution [26], and we refer to [10,16,30] and the references therein for recent progress. The situation is different for the strain gradient elastic model. The well-posedness of the corresponding boundary value problem hinges on a Korn-like inequality, which will be dubbed as  $H^2$ -Korn's inequality. Therefore, a discrete  $H^2$ -Korn's inequality has to be satisfied for any reasonable nonconforming finite element approximation. We prove a  $H^2$ -Korn's inequality for piecewise vector fields as BRENNER'S seminal  $H^1$  Korn's inequality [9]. Motivated by this discrete Korn's inequality, we propose two nonconforming  $H^2$ -finite elements, which are  $H^1$ -conforming. Both elements satisfy the discrete  $H^2$ -Korn's inequality. We prove that both elements converge in energy norm uniformly with respect to the small perturbation parameter. Numerical results also confirm the theoretic results.

It is worth mentioning that Soh and Chen [29] constructed several nonconforming finite elements for this strain gradient elastic model. Some of them exhibited excellent numerical performance. Their motivation is the so-called  $C^{0-1}$  patch test, which is obviously different from ours. It is unclear whether their elements are robust with respect to the small perturbation parameter, which may be an interesting topic for further study. As to various numerical methods based on reformulations of the strain gradient elastic model, we refer to [6,31] and the references therein.

The remaining part of the paper is organized as follows. In the next part, we introduce the linear strain gradient elasticity and prove the well-posedness of its Dirichlet boundary value problem by establishing a  $H^2$ -Korn inequality. A discrete  $H^2$ -Korn inequality is proved in Sect. 3, and two finite elements are constructed and analyzed in this part. The numerical results can be found in Sect. 4.

Throughout this paper, the generic constant  $C$  may differ at different occurrences, while it is independent of the microscopic parameter  $\iota$  and the mesh size  $h$ .

## 55 2 The Korn's inequality of strain gradient elasticity

56 The space  $L^2(\Omega)$  of the square-integrable functions defined on a bounded polygon  
57  $\Omega$  is equipped with the inner product  $(\cdot, \cdot)$  and the norm  $\|\cdot\|_{L^2(\Omega)}$ . Let  $H^m(\Omega)$  be the  
58 standard Sobolev space [1] and

$$59 \quad \|v\|_{H^m(\Omega)} = \sum_{k=0}^m |v|_{H^k(\Omega)}^2 \quad \text{and} \quad |v|_{H^k(\Omega)}^2 = \int_{\Omega} \sum_{|\alpha|=k} |\nabla^\alpha v|^2 dx,$$

60 where  $\alpha = (\alpha_1, \alpha_2)$  is a multi-index whose components  $\alpha_i$  are nonnegative integers,  
61  $|\alpha| = \alpha_1 + \alpha_2$  and  $\nabla^\alpha = \partial^{|\alpha|}/\partial x_1^{\alpha_1} \partial x_2^{\alpha_2}$ . We may drop  $\Omega$  in the Sobolev norm  
62  $\|\cdot\|_{H^m(\Omega)}$  when there is no confusion may occur. The space  $H_0^m(\Omega)$  is the closure in  
63  $H^m(\Omega)$  of  $C_0^\infty(\Omega)$ . In particular,

$$64 \quad H_0^1(\Omega) := \{v \in H^1(\Omega) \mid v = 0 \text{ on } \partial\Omega\},$$

$$65 \quad H_0^2(\Omega) := \{v \in H^1(\Omega) \mid v = \partial_n v = 0 \text{ on } \partial\Omega\},$$

67 where  $\partial_n v$  is the normal derivative of  $v$ . Equally,  $\partial_t v$  denotes the tangential derivative  
68 of  $v$ . The summation convention is used for repeated indices. A comma followed by a  
69 subscript, say  $i$ , denotes partial differentiation with respect to the spatial variables  $x_i$ ,  
70 i.e.,  $v_{,i} = \partial v / \partial x_i$ .

71 For any vector-valued function  $v$ , its gradient is a matrix-valued function with  
72 components  $(\nabla v)_{ij} = \partial v_i / \partial x_j$ . The symmetric part of a gradient field is also a  
73 matrix-valued function defined by

$$74 \quad \epsilon(v) = \frac{1}{2} (\nabla v + [\nabla v]^T).$$

75 The anti-symmetric part of a gradient field is defined as  $\nabla^a v = \nabla v - \epsilon(v)$ . The  
76 divergence operator applying to a vector field is defined as the trace of  $\nabla v$ , i.e.,  $\nabla \cdot v =$   
77  $\text{tr} \nabla v = \partial v_i / \partial x_i$ . The Sobolev spaces  $[H^m(\Omega)]^2$ ,  $[H_0^m(\Omega)]^2$  and  $[L^2(\Omega)]^2$  of a vector  
78 field can be defined in a similar manner as their scalar counterparts, this rule equally  
79 applies to their inner products and their norms. For the  $m$ -th order tensors  $A$  and  $B$ ,  
80 we define the inner product as  $A:B = \sum_{i_1, \dots, i_m} A_{i_1} B_{i_1} \dots A_{i_m} B_{i_m}$ .

### 81 2.1 Strain gradient elastic model and $H^2$ -Korn inequality

82 The strain gradient elastic model in [3, 14, 28] is described by the following boundary  
83 value problem: For  $u$  the displacement vector that solves

$$84 \quad \begin{cases} (\iota^2 \Delta - I) (\mu \Delta u + (\lambda + \mu) \nabla \nabla \cdot u) = f, & \text{in } \Omega, \\ u = \partial_n u = 0, & \text{on } \partial\Omega. \end{cases} \quad (1)$$

85 Here  $\lambda$  and  $\mu$  are the Lamé constants, and  $\iota$  is the microscopic parameter such that  
86  $0 < \iota \leq 1$ . In particular, we are interested in the regime when  $\iota$  is close to zero.

87 The above boundary value problem may be rewritten into the following variational  
88 problem: Find  $u \in [H_0^2(\Omega)]^2$  such that

$$89 \quad a(u, v) = (f, v) \quad \text{for all } v \in [H_0^2(\Omega)]^2, \quad (2)$$

90 where

$$91 \quad a(u, v) = (\mathbb{C}\epsilon(u), \epsilon(v)) + (\mathbb{D}\nabla\epsilon(u), \nabla\epsilon(v)),$$

92 and the fourth-order tensors  $\mathbb{C}$  and the sixth-order tensor  $\mathbb{D}$  are defined by

$$93 \quad \mathbb{C}_{ijkl} = \lambda\delta_{ij}\delta_{kl} + 2\mu\delta_{ik}\delta_{jl} \quad \text{and} \quad \mathbb{D}_{ijklmn} = \iota^2 (\lambda\delta_{il}\delta_{jk}\delta_{mn} + 2\mu\delta_{il}\delta_{jm}\delta_{ln}),$$

94 respectively. Here  $\delta_{ij}$  is the Kronecker delta function. The third-order tensor  $\nabla\epsilon(v)$  is  
95 defined as  $(\nabla\epsilon(v))_{ijk} = \epsilon_{jk,i}$ . We only consider the clamped boundary condition in  
96 this paper, the discussion on other boundary conditions can be found in [3, 14, 28].

97 The variational problem (2) is well-posed if and only if the bilinear form  $a(\cdot, \cdot)$  is  
98 coercive over  $[H_0^2(\Omega)]^2$ .

99 **Theorem 1** For any  $v \in [H_0^2(\Omega)]^2$ , there holds

$$100 \quad C(\Omega) \left( \|v\|_{H^1}^2 + \iota^2 |v|_{H^2}^2 \right) \leq a(v, v) \leq 2(\lambda + \mu) \left( \|v\|_{H^1}^2 + \iota^2 |v|_{H^2}^2 \right), \quad (3)$$

101 where  $C(\Omega)$  depends only on  $\mu$  and the constant  $C_p$  in the following Poincaré  
102 inequality,

$$103 \quad \|v\|_{L^2} \leq C_p \|\nabla v\|_{L^2}.$$

104 The proof of this theorem essentially depends on the first Korn's inequality [18, 19].  
105 For any  $v \in [H_0^1(\Omega)]^2$ , there holds

$$106 \quad 2\|\epsilon(v)\|_{L^2}^2 \geq \|\nabla v\|_{L^2}^2. \quad (4)$$

107 The proof of this inequality follows from the following identity

$$108 \quad |\epsilon(v)|^2 - |\nabla^a v|^2 = |\nabla \cdot v|^2 + \nabla \cdot [(v \cdot \nabla)v - v(\nabla \cdot v)]$$

109 with the usual notation

$$110 \quad v \cdot \nabla = \sum_{i=1}^2 v_i \frac{\partial}{\partial x_i}.$$

111 Indeed, by the fact  $v = 0$  on  $\partial\Omega$ , the above identity and divergence theorem imply

$$112 \quad \int_{\Omega} |\nabla^a v|^2 dx = \int_{\Omega} |\epsilon(v)|^2 dx - \int_{\Omega} |\nabla \cdot v|^2 dx \leq \int_{\Omega} |\epsilon(v)|^2 dx,$$

113 which implies the first Korn's inequality (4) by using the algebraic identity

$$114 \quad |\nabla v|^2 = |\epsilon(v)|^2 + |\nabla^a v|^2.$$

115 *Proof of Theorem 1* By definition, we write

$$116 \quad a(v, v) = 2\mu \|\epsilon(v)\|_{L^2}^2 + \lambda \|\nabla \cdot v\|_{L^2}^2 + \iota^2 \left( 2\mu \|\nabla \epsilon(v)\|_{L^2}^2 + \lambda \|\nabla \nabla \cdot v\|_{L^2}^2 \right).$$

117 The upper bound in (3) immediately follows by noting

$$118 \quad \|\epsilon(v)\|_{L^2}^2 \leq \|\nabla v\|_{L^2}^2, \quad \text{and} \quad \|\nabla \cdot v\|_{L^2}^2 \leq 2\|\nabla v\|_{L^2}^2.$$

119 For any  $v \in [H_0^2(\Omega)]^2$ , we have  $\partial_i v \in [H_0^1(\Omega)]^2$  for  $i = 1, 2$ , we apply the first  
120 Korn's inequality (4) to the vector field  $\partial_i v$  and obtain

$$121 \quad 2\|\epsilon(\partial_i v)\|_{L^2}^2 \geq \|\nabla \partial_i v\|_{L^2}^2.$$

122 Using the fact that the strain operator  $\epsilon$  and the partial gradient operator  $\partial_i$  commute,  
123 we rewrite the above inequality as

$$124 \quad \begin{aligned} 2\|\nabla \epsilon(v)\|_{L^2}^2 &= 2 \sum_{i=1}^2 \|\partial_i \epsilon(v)\|_{L^2}^2 = 2 \sum_{i=1}^2 \|\epsilon(\partial_i v)\|_{L^2}^2 \\ 125 \quad &\geq \sum_{i=1}^2 \|\nabla \partial_i v\|_{L^2}^2 = \|\nabla^2 v\|_{L^2}^2. \end{aligned}$$

126 Therefore,

$$127 \quad a(v, v) \geq \mu \left( |v|_{H^1}^2 + \iota^2 |v|_{H^2}^2 \right),$$

128 which together with the *Poincaré* inequality leads to the lower bound in (3).  $\square$

129 Proceeding along the same line in [26, §5], we may prove the following regularity  
130 results for the solution of Problem (2).

131 **Lemma 1** *There exists  $C$  that may depend on  $\Omega$  but independent of  $\iota$  such that*

$$132 \quad |u|_{H^2} + \iota |u|_{H^3} \leq C \iota^{-1/2} \|f\|_{L^2}, \quad (5)$$

133 and

$$134 \quad \|u - u^0\|_{H^1} \leq C \iota^{1/2} \|f\|_{L^2}, \quad (6)$$

135 where  $u^0 \in [H_0^1(\Omega)]^2$  satisfies

$$136 \quad (\mathbb{C}\epsilon(u^0), \epsilon(v)) = (f, v) \quad \text{for all } v \in [H_0^1(\Omega)]^2. \quad (7)$$

### 3 The nonconforming finite elements

In this part, we introduce two nonconforming finite elements to approximate the variational problem (2). Let  $\mathcal{T}_h$  be a triangulation of  $\Omega$  with maximum mesh size  $h$ . We assume all elements in  $\mathcal{T}_h$  is shape-regular in the sense of Ciarlet and Raviart [11]. Denote the set of all the edges in  $\mathcal{T}_h$  as  $\mathcal{S}(\Omega, \mathcal{T}_h)$ . The space of piecewise  $[H^m(\Omega, \mathcal{T}_h)]^2$  vector fields is defined by

$$[H^m(\Omega, \mathcal{T}_h)]^2 := \{v \in [L^2(\Omega)]^2 \mid v|_T \in [H^m(T)]^2, \quad \forall T \in \mathcal{T}_h\},$$

which is equipped with the broken norm

$$\|v\|_{H_h^k} := \|v\|_{L^2} + \sum_{k=1}^m \|\nabla_h^k v\|_{L^2},$$

where

$$\|\nabla_h^k v\|_{L^2}^2 = \sum_{T \in \mathcal{T}_h} \|\nabla^k v\|_{L^2(T)}^2$$

with  $(\nabla_h^k v)|_T = (\nabla^k v)|_T$ . Moreover,  $\epsilon_h(v) = (\nabla_h v + [\nabla_h v]^T)/2$ .

Brenner [9] established a discrete Korn inequality for any piecewise  $H^1$  vector fields with weak linear continuity across the common surface between two adjacent elements, i.e., for any  $v \in [H^1(\Omega, \mathcal{T}_h)]^d$  with  $d = 2, 3$  satisfying

$$\int_e \llbracket v \rrbracket \cdot p \, d\tau = 0, \quad p \in [P_1(e)]^d, \quad e \in \mathcal{S}(\Omega, \mathcal{T}_h).$$

There exists a constant  $C$  depends on  $\Omega$  and  $\mathcal{T}_h$  but independent of  $h$  such that

$$\|v\|_{H_h^1} \leq C (\|v\|_{L^2} + \|\epsilon_h(v)\|_{L^2}). \quad (8)$$

Here  $[P_1(e)]^d$  is the linear vector field over  $e$  and  $\llbracket v \rrbracket$  denotes the jump of  $v$  across  $e$  with  $e$  an edge for  $d = 2$  and a face for  $d = 3$ . This inequality is fundamental to the well-posedness of the discrete problems arising from nonconforming finite element and discontinuous Galerkin method approximation of the linearized elasticity model and Reissner–Mindlin plate model; See [15, 25] and [17].

Mardal and Winther [21] improved the above inequality by replacing  $[P_1(e)]^d$  by its subspace  $[P_{1,-}(e)]^d$  given by

$$[P_{1,-}(e)]^d := \{v \in [P_1(e)]^d \mid v \cdot t \in \text{RM}(e)\},$$

where  $t$  is the tangential vector of edge  $e$ , and  $\text{RM}(e)$  is the infinitesimal rigid motion on  $e$ . In fact, they have proved

$$|v|_{H_h^1}^2 \leq C \left( \|\epsilon_h(v)\|_{L^2}^2 + \|v\|_{L^2}^2 + \sum_{e \in \mathcal{S}(\Omega, \mathcal{T}_h)} h_e^{-1} \|\llbracket \Pi_e v \rrbracket\|_{L^2(e)}^2 \right), \quad (9)$$

where  $\Pi_e : [L^2(e)]^d \mapsto [P_{1,-}(e)]^d$  is the  $L^2$  projection.

Our result is an  $H^2$  analog of the discrete Korn's inequality (9).

**Theorem 2** For any  $v \in [H^2(\Omega, \mathcal{T}_h)]^2$ , there exists  $C$  that depends on  $\Omega$  and  $\mathcal{T}_h$  but independent of  $h$  such that

$$\begin{aligned} \|v\|_{H_h^2}^2 &\leq C \left( \|\nabla_h \epsilon_h(v)\|_{L^2}^2 + \|\epsilon_h(v)\|_{L^2}^2 + \|v\|_{L^2}^2 + \sum_{e \in \mathcal{S}(\Omega, \mathcal{T}_h)} h_e^{-1} \|\llbracket \Pi_e v \rrbracket\|_{L^2(e)}^2 \right. \\ &\quad \left. + \sum_{i=1}^2 \sum_{e \in \mathcal{S}(\Omega, \mathcal{T}_h)} h_e^{-1} \|\llbracket \Pi_e(\partial_i v) \rrbracket\|_{L^2(e)}^2 \right). \end{aligned} \quad (10)$$

The proof follows essentially the same line that leads to Theorem 1.

*Proof* For any  $v \in [H^2(\Omega, \mathcal{T}_h)]^2$ , it is clear that  $\partial_i v \in [H^1(\Omega, \mathcal{T}_h)]^2$  for  $i = 1, 2$ .

Applying the discrete Korn's inequality (9) to each  $\partial_i v$ , we obtain

$$\begin{aligned} |v|_{H_h^2}^2 &= |\partial_1 v|_{H_h^1}^2 + |\partial_2 v|_{H_h^1}^2 \\ &\leq C \sum_{i=1}^2 \left( \|\epsilon_h(\partial_i v)\|_{L^2}^2 + \|\partial_i v\|_{L^2}^2 + \sum_{e \in \mathcal{S}(\Omega, \mathcal{T}_h)} h_e^{-1} \|\llbracket \Pi_e(\partial_i v) \rrbracket\|_{L^2(e)}^2 \right) \\ &= C \left( \|\nabla_h \epsilon_h(v)\|_{L^2}^2 + \|\nabla_h v\|_{L^2}^2 + \sum_{i=1}^2 \sum_{e \in \mathcal{S}(\Omega, \mathcal{T}_h)} h_e^{-1} \|\llbracket \Pi_e(\partial_i v) \rrbracket\|_{L^2(e)}^2 \right). \end{aligned}$$

Invoking (9) once again, we get (10).  $\square$

Motivated by the discrete Korn's inequality (10), we construct two new finite elements that are  $H^1$ -conforming but  $H^2$ -nonconforming elements. For such elements, the continuity of the tangential derivatives are automatically satisfied, and we only need to deal with the weak continuity of the normal derivative. The finite element space is defined as

$$V_h := \{ v \in [H_0^1(\Omega)]^2 \mid v|_T \in W(T) \text{ for all } T \in \mathcal{T}_h \}.$$

We shall specify two local finite element spaces  $W(T)$  in the next two parts.

Given  $V_h$ , we find  $u_h \in V_h$  such that

$$a_h(u_h, v) = (f, v) \quad \text{for all } v \in V_h, \quad (11)$$

where the bilinear form  $a_h$  is defined for any  $v, w \in V_h$  as

$$a_h(v, w) := (C\epsilon(v), \epsilon(w)) + (\mathbb{D}\nabla_h \epsilon(v), \nabla_h \epsilon(w)),$$

190 where the second term is defined in a piecewise manner as

$$191 \quad (\mathbb{D}\nabla_h\epsilon(v), \nabla_h\epsilon(w)) := \sum_{T \in \mathcal{T}_h} \int_T \mathbb{D}\nabla\epsilon(v)\nabla\epsilon(w) \, dx.$$

### 192 3.1 The first nonconforming element

193 Define

$$194 \quad W(T) := [P_2(T)]^2 \oplus bP_2^*(T), \tag{12}$$

195 where  $P_2(T)$  is the quadratic Lagrange element, and  $b = \lambda_1\lambda_2\lambda_3$  is the cubic bubble  
 196 function, and  $P_2^*(T) \subset [P_2(T)]^2$  is defined as

$$197 \quad P_2^*(T) := \{ v \in [P_2(T)]^2 \mid v \cdot n|_e \in P_1(e) \text{ for all } e \in \partial T \}.$$

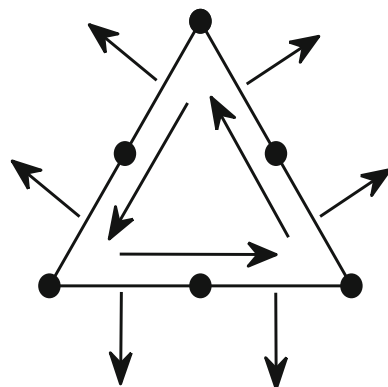
198 Next lemma gives the degrees of freedom of this element, which is graphically  
 199 shown in Fig. 1, and we prove that the degrees of freedom is  $W(T)$ –unisolvent.

200 **Lemma 2** *The dimension of  $W(T)$  is 21. Any  $w \in W(T)$  is uniquely determined by*  
 201 *the following degrees of freedom:*

- 202 1. *The values of  $w$  at the corners and edge midpoints;*
- 203 2. *The moments  $\int_e \partial_n(w \cdot t) \, d\tau$  and  $\int_e \partial_n(w \cdot n)\tau^k \, d\tau$  for  $k = 0, 1$  and for all  $e \in \partial T$ .*

204 *Proof* Since  $[P_2(T)]^2 \cap bP_2^*(T) = \{0\}$  and  $\dim P_2^*(T) \geq 9$ , we conclude  
 205  $\dim W(T) \geq 21$ . It suffices to show that a function  $w \in W(T)$  vanishes if all  
 206 the degrees of freedom are zeros. Note that  $w|_e \in [P_2(e)]^2$ , with three roots on edge  
 207  $e$ , then we must have  $w|_{\partial T} = 0$ . Therefore, we may write  $w = bp$  with  $p \in P_2^*(T)$ .  
 208 Let  $e$  be a fixed edge of  $T$ , and denote  $b = \lambda_e\lambda_+\lambda_-$  with  $\lambda_e$  the barycentric coordinate  
 209 functions such that  $\lambda_e \equiv 0$  on  $e$ , while  $\lambda_+$  and  $\lambda_-$  the remaining two barycentric

**Fig. 1** The degrees of freedom are point evaluations at the vertex and midpoint of each edge, are the moments of the normal derivative of the normal component against  $P_1$  over each edge, are the moments of the normal derivative of the tangential component along each edge



Author Proof



coordinate functions. Furthermore,  $(\nabla w)|_e = (p\lambda_+\lambda_-)|_e \nabla \lambda_e$ . Note that  $\lambda_+\lambda_-\partial_n \lambda_e$  is strictly negative in the interior of  $e$ . Therefore, the condition

$$0 = \int_e \partial_n(w \cdot n) \tau^k \, d\tau = \int_e \lambda_+\lambda_- \frac{\partial \lambda_e}{\partial n} p \cdot n \tau^k \, d\tau$$

implies that for any  $e \in \partial T$  and  $k = 0, 1$ ,

$$\int_e p \cdot n \tau^k \, d\tau = 0. \quad (13)$$

Proceeding along the same line, we obtain, for any  $e \in \partial T$ ,

$$\int_e p \cdot t \, d\tau = 0. \quad (14)$$

Furthermore, using the fact that  $p \cdot n \in P_1(e)$  and (13), we conclude that  $p \cdot n \equiv 0$  over  $\partial T$ .

Assume that

$$p = \left( \sum_{|\alpha|=2} a_\alpha \lambda_1^{\alpha_1} \lambda_2^{\alpha_2} \lambda_3^{\alpha_3}, \sum_{|\alpha|=2} b_\alpha \lambda_1^{\alpha_1} \lambda_2^{\alpha_2} \lambda_3^{\alpha_3} \right)^T,$$

where  $\alpha = (\alpha_1, \alpha_2, \alpha_3)$  whose components  $\alpha_i$  are nonnegative integers and  $|\alpha| = \alpha_1 + \alpha_2 + \alpha_3$ .

Using  $(p \cdot n_i)|_{e_i} \equiv 0$ , we obtain, for  $j = 1, 2, 3$ ,

$$(a_\alpha, b_\alpha) \cdot n_j = 0 \quad \text{with} \quad \alpha_j = 0. \quad (15)$$

This means that, for each  $\alpha$  with one component equals to 2, the vector  $(a_\alpha, b_\alpha)$  is orthogonal to the normal directions of two different edges, which immediately implies that such vector  $(a_\alpha, b_\alpha)$  must be zero.

Next, using the fact that  $\int_{e_i} (p \cdot t) \, d\tau \equiv 0$ , we obtain, for  $j = 1, 2, 3$ ,

$$(a_\alpha, b_\alpha) \cdot t_j = 0, \quad \text{with} \quad \alpha_j = 0, \alpha_k = 1 \quad \text{for} \quad k \neq j.$$

Invoking (15) once again, we conclude that, for each  $\alpha$  with only one zero component,  $(a_\alpha, b_\alpha)$  is orthogonal to both the normal direction and the tangential direction of the edge indexed with the zero component of  $\alpha$ , which must vanish identically. Therefore, all  $a_\alpha$  and  $b_\alpha$  are zeros, and hence  $p \equiv 0$ , equivalently,  $w \equiv 0$ . This completes the proof.  $\square$

Using the degrees of freedom given in Lemma 2, we may define a local interpolation operator  $\Pi_T : H^2(T) \mapsto W(T)$ . The next lemma shows that this operator locally preserves quadratics.

**Lemma 3**

$$\Pi_T v = v, \quad v \in [P_2(T)]^2. \quad (16)$$

*Proof* Let  $(T, W(T), \Sigma(T))$  be the finite element triple with  $\Sigma(T)$  the degrees of freedom. By construction,  $\Sigma(T)$  takes the form as

$$\Sigma(T) = \{d_1^{(l)}, \dots, d_{12}^{(l)}, d_1^{(m)}, \dots, d_9^{(m)}\},$$

where  $\{d_i^{(l)}\}_{i=1}^{12}$  are the nodal type degrees of freedom, and  $\{d_i^{(m)}\}_{i=1}^9$  are the moment type degrees of freedom. The basis functions for  $[P_2(T)]^2$  and  $bP_2^*(T)$  are denoted by  $\{\phi_i\}_{i=1}^{12}$  and  $\{\psi_i\}_{i=1}^9$ , respectively.

Define a new set of basis functions

$$\varphi_i = \phi_i - \sum_{j=1}^9 d_j^{(m)}(\phi_i) \psi_j, \quad i = 1, \dots, 12.$$

We claim

$$W(T) = \text{span}\{\varphi_1, \dots, \varphi_{12}, \psi_1, \dots, \psi_9\}. \quad (17)$$

Note that  $d_i^{(l)}(\psi_j) \equiv 0$  because  $\psi_j = 0$  on  $\partial T$ . We obtain  $\{\psi_j\}_{j=1}^9$  are the basis functions of  $W(T)$  associated with the degrees of freedom  $\{d_j^{(m)}\}_{j=1}^9$ . For any  $\varphi_i$ , there holds

$$d_j^{(l)}(\varphi_i) = d_j^{(l)}(\phi_i) - \sum_{k=1}^9 d_k^{(m)}(\phi_i) d_j^{(l)}(\psi_k) = d_j^{(l)}(\phi_i) = \delta_{ij},$$

and

$$\begin{aligned} d_j^{(m)}(\varphi_i) &= d_j^{(m)}(\phi_i) - \sum_{k=1}^9 d_k^{(m)}(\phi_i) d_j^{(m)}(\psi_k) \\ &= d_j^{(m)}(\phi_i) - \sum_{k=1}^9 d_k^{(m)}(\phi_i) \delta_{jk} = 0. \end{aligned}$$

This verifies the claim (17).

Next, we prove the interpolation operator is locally  $P_2$  invariant. For any  $v \in [P_2(T)]^2$ , we have the representation

$$v = \sum_{i=1}^{12} d_i^{(l)}(v) \phi_i.$$

261 By definition,

$$\begin{aligned}
 262 \quad \Pi_T v &= \sum_{i=1}^{12} d_i^{(l)}(v) \phi_i + \sum_{j=1}^9 d_j^{(m)}(v) \psi_j \\
 263 \quad &= \sum_{i=1}^{12} d_i^{(l)}(v) \phi_i - \sum_{j=1}^9 \sum_{i=1}^{12} d_i^{(l)}(v) d_j^{(m)}(\phi_i) \psi_j + \sum_{j=1}^9 d_j^{(m)}(v) \psi_j \\
 264 \quad &= \sum_{i=1}^{12} d_i^{(l)}(v) \phi_i - \sum_{j=1}^9 \left( \sum_{i=1}^{12} d_i^{(l)}(v) d_j^{(m)}(\phi_i) - d_j^{(m)}(v) \right) \psi_j \\
 265 \quad &= \sum_{i=1}^{12} d_i^{(l)}(v) \phi_i = v, \\
 266
 \end{aligned}$$

267 where we have used the identity

$$268 \quad d_j^{(m)}(v) = d_j^{(m)} \left( \sum_{i=1}^{12} d_i^{(l)}(v) \phi_i \right) = \sum_{i=1}^{12} d_i^{(l)}(v) d_j^{(m)}(\phi_i).$$

269 This completes the proof.  $\square$

270 The above proof actually provides a constructive way to derive the basis function  
271 of this element.

### 272 3.2 The second nonconforming element

273 The second element is almost the same with the first one except that  $P_2^*$  is replaced  
274 by

$$275 \quad P_3^*(T) = \{ w \in [P_3(T)]^2 \mid \nabla \cdot w \in P_0(T), w \cdot n|_e \in P_1(e) \text{ for all } e \in \partial T \}.$$

276 Hence,

$$277 \quad W(T) = [P_2(T)]^2 \oplus bP_3^*(T). \quad (18)$$

278 Here  $P_3^*(T)$  has appeared in [22] to solve Darcy-Stokes flow.

279 The following lemma gives the degrees of freedom of this element, and we prove  
280 it is  $W(T)$ -unisolvent.

281 **Lemma 4** *The dimension of  $W(T)$  is 21. Any  $w \in W(T)$  is uniquely determined by*  
282 *the following degrees of freedom:*

- 283 1. *The values of  $w$  at the corners and edge midpoints;*
- 284 2. *The moments  $\int_e \partial_n(w \cdot t) \, \tau$  and  $\int_e \partial_n(w \cdot n) \tau^k \, \tau$  for  $k = 0, 1$  and for all  $e \in \partial T$ .*

285 The proof of this result is slightly different from the direct proof of Lemma 2.

286 *Proof* Proceeding along the same line that leads to (13) and (14), we obtain that for  
 287 all  $e \in \partial T$ ,

$$288 \int_e p \cdot n \tau^k d\tau = 0, k = 0, 1, \quad \text{and} \quad \int_e p \cdot t d\tau = 0. \quad (19)$$

289 Using the fact that  $(p \cdot n)|_{\partial T} \in P_1$  and the first identity of (19), we conclude that  
 290  $(p \cdot n)|_{\partial T} \equiv 0$ , which immediately implies

$$291 \int_T \nabla \cdot p dx = \int_{\partial T} p \cdot n d\tau = 0.$$

292 Since  $\nabla \cdot p \in P_0(T)$ , this implies that  $p$  is divergence free. Then there exists a  
 293 polynomial  $\phi \in P_4(T)$  such that  $p = \text{curl}\phi$ . Furthermore, since

$$294 \partial_\tau \phi|_{\partial T} = p \cdot n|_{\partial T} = 0,$$

295 which implies that  $\phi$  is constant along the edge of  $T$ . Without loss of generality, we  
 296 assume that  $\phi|_{\partial T} \equiv 0$ . Hence,  $\phi$  is of the form  $\phi = b\varphi$  with  $\varphi \in P_1(T)$ . By the  
 297 second identity of (19), we obtain

$$298 \int_e \partial_n \phi d\tau = \int_e p \cdot t d\tau = 0.$$

299 Note that  $\partial_n \phi|_e = \lambda_+ \lambda_- \partial_n \lambda_e \varphi|_e$  and the fact that  $\lambda_+ \lambda_- \partial_n \lambda_e$  is strictly negative in  
 300 the interior of the edge  $e$ , we conclude that  $\varphi$  has a root at each edge, which together  
 301 with the fact that  $\varphi \in P_1(T)$  yields  $\varphi \equiv 0$ , or equivalently  $w = 0$ . This completes the  
 302 proof.  $\square$

303 Proceeding along the same line that leads to (16), we conclude that this noncon-  
 304 forming element also locally preserves quadratics.

305 *Remark 1* Both elements are endowed with the same degrees of freedom. The structure  
 306 of the local finite element spaces for both element are similar. In fact, the bubble  
 307 functions can be removed by standard static condensation procedure. Therefore, the  
 308 resulting method has only 12 degrees of freedom on each element.

309 For any function  $v \in V_h$ , we obtain a simplified version of the discrete Korn's  
 310 inequality (10) without all the jump terms, which may be regarded as a  $H^2$ - analog  
 311 of the discrete Korn's inequality (8).

312 **Lemma 5** *There exists  $C$  depends on  $\Omega$  and  $\mathcal{T}_h$ , but independent of  $h$  such that*

$$313 \|v\|_{H_h^2} \leq C (\|\nabla_h \epsilon(v)\|_{L^2} + \|\epsilon(v)\|_{L^2}). \quad (20)$$

314 *Proof* For any function  $v \in V_h$ , we claim that the jump terms in the right-hand side  
 315 of (10) vanish. Indeed,  $[[\Pi_e v]] = 0$  for any  $e \in \mathcal{S}(\Omega, \mathcal{T}_h)$  because  $v \in [H_0^1(\Omega)]^2$ . It  
 316 remains to verify that for all  $e \in \mathcal{S}(\Omega, \mathcal{T}_h)$  and  $i = 1, 2$ ,

317 
$$[[\Pi_e(\partial_i v)]] = 0. \tag{21}$$

318 We write  $\partial_i v = \alpha_i \partial_n v + \beta_i \partial_t v$ , where  $\alpha_i$  and  $\beta_i$  are constants. Hence, it remains to  
 319 show

320 
$$[[\Pi_e(\partial_n v)]] = 0, \quad [[\Pi_e(\partial_t v)]] = 0, \quad \forall e \in \mathcal{S}(\Omega, \mathcal{T}_h).$$

321 Since  $V_h$  is  $H^1$ -conforming, it is clear that  $[[\Pi_e(\partial_t v)]] = 0$ .

322 For any  $e \in \mathcal{S}(\Omega, \mathcal{T}_h)$ , it is clear that  $RM(e) = P_0(e)$ . For any  $w \in [P_{1,-}(e)]^2$ ,  
 323 there holds

324 
$$w = w_n n + w_t t, \quad w_n \in P_1(e), w_t \in P_0(e).$$

325 Hence,  $[[\Pi_e(\partial_n v)]] = 0$ , if and only if

326 
$$\int_e [[\partial_n(v \cdot n)]] \tau^k d\tau = 0, k = 0, 1, \quad \text{and} \quad \int_e [[\partial_n(v \cdot t)]] d\tau = 0.$$

327 This is true for any  $v \in W(T)$  and we prove the claim (21).

328 For any  $v \in V_h$ , it follows from (10) that

329 
$$\|v\|_{H_h^2} \leq C (\|\nabla_h \epsilon(v)\|_{L^2} + \|\epsilon(v)\|_{L^2} + \|v\|_{L^2}).$$

330 The inequality (20) follows by using the Poincaré’s inequality and the first Korn’s  
 331 inequality (4):

332 
$$\|v\|_{L^2}^2 \leq C_p^2 \|\nabla v\|_{L^2}^2 \leq 2C_p^2 \|\epsilon(v)\|_{L^2}^2.$$

333 □

334 We are ready to prove the coercivity of the bilinear form  $a_h$  over  $V_h$ .

335 **Theorem 3** For any  $\iota < 1/\sqrt{2}$ , there exists  $C$  that depends on the domain  $\Omega$  and the  
 336 shape regularity of the triangulation  $\mathcal{T}_h$  such that

337 
$$a_h(v, v) \geq C(\iota^2 \|v\|_{H_h^2}^2 + \|v\|_{H^1}^2), \quad \forall v \in V_h. \tag{22}$$

338 *Proof* For any  $v \in V_h$ , using (20), we obtain, there exists  $C$  that is independent of  $h$   
 339 such that

340 
$$\begin{aligned} a_h(v, v) &\geq 2\mu \left( \iota^2 \|\nabla_h \epsilon(v)\|_{L^2}^2 + \|\epsilon(v)\|_{L^2}^2 \right) \\ &\geq 2\mu \iota^2 \left( \|\nabla_h \epsilon(v)\|_{L^2}^2 + \|\epsilon(v)\|_{L^2}^2 \right) + \mu \|\epsilon(v)\|_{L^2}^2 \\ &\geq C \left( \iota^2 \|v\|_{H_h^2}^2 + \|v\|_{H^1}^2 \right), \end{aligned}$$

341  
342  
343

Author Proof

344 which implies (22), where we have used

$$345 \quad \|v\|_{H^1}^2 = \|v\|_{L^2}^2 + \|\nabla v\|_{L^2}^2 \leq (C_p^2 + 1)\|\nabla v\|_{L^2}^2 \leq 2(C_p^2 + 1)\|\epsilon(v)\|_{L^2}^2,$$

346 in the last step.  $\square$

347 The following interpolate estimate is a direct consequence of the quadratics invari-  
348 ance of the local finite element spaces  $W(T)$ ; The proof is standard, and we refer  
349 to [12] for the details.

350 **Lemma 6** *There exists  $C$  independent of  $h$  such that for all  $v \in [H^k(T)]^2$ ,*

$$351 \quad \|v - \Pi_T v\|_{H^j(T)} \leq Ch^{k-j}|v|_{H^k(T)}, \quad j = 0, 1, 2, k = 2, 3. \quad (23)$$

352 A global interpolation operator  $I_h : H^k(\Omega) \mapsto V_h$  is defined by  $(I_h)|_T = \Pi_T$ .

### 353 3.3 Convergence analysis

354 We are ready to prove the main result of this paper.

355 **Theorem 4** *Assume that the weak solution of  $u$  of the problem (2) belongs to*  
356  *$[H_0^2(\Omega)]^2 \cap [H^3(\Omega)]^2$ . Let  $u_h$  be the solution of (11). Then there exists  $C$  independent*  
357 *of  $\iota$  and  $h$  such that*

$$358 \quad \|u - u_h\|_{\iota, h} \leq \begin{cases} C(h^2 + \iota h)|u|_{H^3}, \\ Ch(|u|_{H^2} + \iota|u|_{H^3}), \end{cases} \quad (24)$$

359 where  $\|v\|_{\iota, h}^2 := a_h(v, v)$  for any  $v \in V_h$ .

360 *Proof* By the the theorem of Berger, Scott, and Strang [8], we have

$$361 \quad \|u - u_h\|_{\iota, h} \leq \inf_{v \in V_h} \|u - v\|_{\iota, h} + \sup_{w \in V_h} \frac{E_h(u, w)}{\|w\|_{\iota, h}}, \quad (25)$$

362 where  $E_h(u, w) = a_h(u, w) - (f, w)$ .

363 By the interpolate estimate (23), we obtain

$$364 \quad \inf_{v \in V_h} \|u - v\|_{\iota, h} \leq \|u - I_h u\|_{\iota, h} \leq \begin{cases} C(h^2 + \iota h)|u|_{H^3}, \\ Ch(|u|_{H^2} + \iota|u|_{H^3}). \end{cases} \quad (26)$$

365 Next, we focus on the estimate of the consistency error. We write  $\kappa_{ijk} =$   
366  $(\nabla \epsilon(u))_{ijk} = \partial_{x_i} \epsilon_{jk}(u)$ . The stress and couple stress are defined by  $\sigma = \mathbb{C}\epsilon(u)$   
367 and  $\tau = \mathbb{D}\nabla \epsilon(u)$ , respectively. Or

$$368 \quad \sigma_{ij} = \mathbb{C}_{ijkl}\epsilon_{kl}(u) \quad \text{and} \quad \tau_{ijk} = \mathbb{D}_{ijklmn}\kappa_{lmn}(u).$$

369 By the symmetry of the tensors  $\mathbb{C}$  and  $\mathbb{D}$ , there holds

370 
$$\sigma_{ij} = \sigma_{ji} \quad \text{and} \quad \tau_{ijk} = \tau_{ikj}.$$

371 By the chain rule and the symmetry of  $\mathbb{C}$  and  $\mathbb{D}$ , we obtain, on each element  $T$  and  
 372 for any  $w \in V_h$ ,

373 
$$\begin{aligned} \mathbb{C}\epsilon(u) : \epsilon(w) + \mathbb{D}\nabla\epsilon(u) : \nabla\epsilon(w) &= \sigma_{jk}\epsilon_{jk}(w) + \tau_{ijk}\kappa_{ijk}(w) \\ &= \sigma_{jk}w_{k,j} + \tau_{ijk}w_{k,ij} \\ &= ((\sigma_{jk} - \tau_{ijk,i})w_k)_{,j} - (\sigma_{jk,j} - \tau_{ijk,ij})w_k \\ &\quad + (\tau_{ijk}w_{k,j})_{,i}. \end{aligned}$$

378 Using the above representation and integration by parts, we obtain

379 
$$\begin{aligned} &\int_T \mathbb{C}\epsilon(u) : \epsilon(w) + \mathbb{D}\nabla\epsilon(u) : \nabla\epsilon(w) \, dx \\ &= \int_T (\tau_{ijk,ij} - \sigma_{jk,j})w_k \, dx \\ &\quad + \int_{\partial T} n_j(\sigma_{jk} - \tau_{ijk,i})w_k \, d\tau + \int_{\partial T} n_i\tau_{ijk}w_{k,j} \, d\tau. \end{aligned} \tag{27}$$

380 Using the fact  $w_{k,j} = n_j\partial_n w_k + t_j\partial_t w_k$  and

381 
$$n_i t_j \tau_{ijk} \partial_t w_k = \partial_t (n_i t_j \tau_{ijk} w_k) - \partial_t (n_i t_j \tau_{ijk}) w_k,$$

382 we obtain

383 
$$\int_{\partial T} n_i \tau_{ijk} w_{k,j} \, d\tau = \int_{\partial T} n_i n_j \tau_{ijk} \partial_n w_k \, d\tau - \int_{\partial T} (n_i t_j \tau_{ijk}) w_k \, d\tau, \tag{28}$$

384 where we have used the fact that the contour integration of tangential derivative along  
 385 the element boundary is zero. By (27), (28) and the continuity of  $w$ , we obtain

386 
$$\begin{aligned} E_h(u, w) &= \sum_{T \in \mathcal{T}_h} \int_{\partial T} n_i n_j \tau_{ijk} \partial_n w_k \, d\tau \\ &= \sum_{e \in \mathcal{S}(\Omega, \mathcal{T}_h)} \int_e n_i n_j \tau_{ijk} \llbracket \partial_n w_k \rrbracket \, d\tau, \end{aligned}$$

388 where  $\tau_{ijk} = \iota^2 \sigma_{jk,i}$ .

389 By

390 
$$\int_e \llbracket \partial_n (w \cdot n) \rrbracket \, d\tau = 0 \quad \text{and} \quad \int_e \llbracket \partial_n (w \cdot t) \rrbracket \, d\tau = 0,$$

we obtain, for  $k = 1, 2$ ,

$$\int_e \llbracket \partial_n w_k \rrbracket d\tau = 0.$$

Employing the standard trace inequality and scaling argument, we obtain

$$|E_h(u, w)| \leq Ch|\tau|_{H^1} |\partial_n w|_{H_h^1} \leq Ct^2 h |u|_{H^3} |w|_{H_h^2}.$$

Substituting the above estimate and (26) into (25), we obtain (24).  $\square$

Combining the error estimate (24) and the regularity results in Lemma 1, proceeding along the same line of [26, Theorem 5.2], we could obtain the following  $\iota$ -independent error estimate

$$\|u - u_h\|_{\iota, h} \leq Ch^{1/2} \|f\|_{L^2}, \quad (29)$$

where  $C$  is independent of  $\iota$  and  $h$ . We leave the details to the interested readers.

## 4 Numerical example

In this section we provide two numerical examples that show the accuracy of the proposed elements, and the robustness of the elements with respect to the microscopical parameter  $\iota$ . The first example is performed on the uniform mesh, while the second one is performed on the nonuniform mesh. As a first step toward understanding the

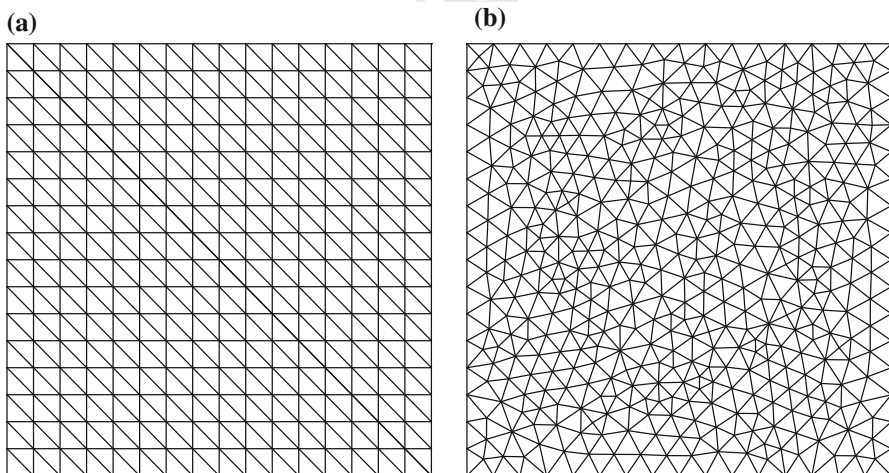


**Fig. 2** Plots of the mesh. **a** Is the uniform triangulations with  $h = 1/16$ . **b** Is the nonuniform mesh with maximum mesh size  $h = 1/16$



**Table 1** The convergence rate of the first element over uniform mesh with  $\lambda = \mu = 1$ 

$\iota \backslash h$	1/16	1/32	1/64	1/128	1/256	1/512
1e0	2.37e-1	1.38e-1	7.31e-2	3.73e-2	1.87e-2	9.38e-3
Rate		0.79	0.91	0.97	0.99	1.00
1e-1	1.81e-1	1.04e-1	5.47e-2	2.78e-2	1.40e-2	6.99e-3
Rate		0.81	0.92	0.98	0.99	1.00
1e-2	3.44e-2	1.66e-2	8.28e-3	4.15e-3	2.07e-3	1.04e-3
Rate		1.06	1.00	1.00	1.00	1.00
1e-3	1.87e-2	5.25e-3	1.54e-3	5.35e-4	2.26e-4	1.07e-4
Rate		1.83	1.77	1.53	1.25	1.08
1e-4	1.85e-2	4.96e-3	1.27e-3	3.22e-4	8.30e-5	2.29e-5
Rate		1.90	1.96	1.98	1.96	1.86
1e-5	1.85e-2	4.95e-3	1.27e-3	3.19e-4	7.98e-5	2.00e-5
Rate		1.90	1.97	1.99	2.00	2.00

**Table 2** The convergence rate of the second element over uniform mesh with  $\lambda = \mu = 1$ 

$\iota \backslash h$	1/16	1/32	1/64	1/128	1/256	1/512
1e0	2.73e-1	1.67e-1	9.22e-2	4.76e-2	2.40e-2	1.20e-2
Rate		0.70	0.86	0.95	0.99	1.00
1e-1	2.10e-1	1.27e-1	6.91e-2	3.55e-2	1.79e-2	8.97e-3
Rate		0.73	0.88	0.96	0.99	1.00
1e-2	4.01e-2	2.04e-2	1.05e-2	5.30e-3	2.66e-3	1.33e-3
Rate		0.97	0.96	0.98	1.00	1.00
1e-3	2.13e-2	6.10e-3	1.83e-3	6.54e-4	2.84e-4	1.36e-4
Rate		1.80	1.74	1.48	1.20	1.06
1e-4	2.10e-2	5.73e-3	1.48e-3	3.75e-4	9.70e-5	2.70e-5
Rate		1.87	1.95	1.98	1.95	1.85
1e-5	2.10e-2	5.73e-3	1.47e-3	3.71e-4	9.29e-5	2.33e-5
Rate		1.87	1.96	1.99	2.00	2.00

size effect of the heterogeneous materials, we test the proposed elements for a benchmark problem with smooth solution. Tests for realistic problems will appear in the forthcoming work.

Let  $\Omega = (0, 1)^2$  and

$$u_1 = (\exp(\cos 2\pi x) - e)(\exp(\cos 2\pi y) - e),$$

$$u_2 = (\cos 2\pi x - 1)(\cos 4\pi y - 1).$$

The force  $f$  is obtained by (1).

**Table 3** The convergence rate of the first element over nonuniform mesh with  $\lambda = \mu = 1$ 

$\iota \backslash h$	1/16	1/32	1/64	1/128	1/256	1/512
1e0	1.26e-1	6.80e-2	3.61e-2	1.87e-2	9.57e-3	4.84e-3
Rate		0.89	0.91	0.94	0.97	0.98
1e-1	9.43e-2	5.08e-2	2.69e-2	1.40e-2	7.14e-3	3.61e-3
Rate		0.89	0.92	0.95	0.97	0.98
1e-2	1.66e-2	7.92e-3	4.05e-3	2.08e-3	1.06e-3	5.35e-4
Rate		1.07	0.97	0.96	0.97	0.99
1e-3	8.24e-3	2.24e-3	6.79e-4	2.52e-4	1.12e-4	5.46e-5
Rate		1.88	1.73	1.43	1.16	1.04
1e-4	8.09e-3	2.09e-3	5.33e-4	1.36e-4	3.56e-5	1.01e-5
Rate		1.95	1.97	1.97	1.94	1.81
1e-5	8.09e-3	2.08e-3	5.31e-4	1.34e-4	3.38e-5	8.48e-6
Rate		1.96	1.97	1.98	1.99	1.99

**Table 4** The convergence rate of the first element over nonuniform mesh with  $\lambda = 10$  and  $\mu = 1$ 

$\iota \backslash h$	1/16	1/32	1/64	1/128	1/256	1/512
1e0	1.09e-1	5.87e-2	3.12e-2	1.63e-2	8.36e-3	4.24e-3
Rate		0.89	0.91	0.94	0.96	0.98
1e-1	8.22e-2	4.43e-2	2.35e-2	1.23e-2	6.30e-3	3.19e-3
Rate		0.89	0.91	0.94	0.96	0.98
1e-2	1.43e-2	6.93e-3	3.58e-3	1.85e-3	9.47e-4	4.79e-4
Rate		1.05	0.96	0.95	0.97	0.98
1e-3	6.67e-3	1.82e-3	5.66e-4	2.18e-4	9.96e-5	4.88e-5
Rate		1.87	1.69	1.38	1.13	1.03
1e-4	6.52e-3	1.67e-3	4.25e-4	1.09e-4	2.87e-5	8.40e-6
Rate		1.97	1.97	1.97	1.92	1.77
1e-5	6.52e-3	1.67e-3	4.23e-4	1.07e-4	2.69e-5	6.75e-6
Rate		1.97	1.98	1.99	1.99	1.99

413 First, the triangulation of the unit square for the uniform mesh is illustrated in  
 414 Fig. 2a. In Tables 1 and 2, we report the convergence rates for both elements in the  
 415 energy norm  $\|u - u_h\|_{\iota, h} / \|u\|_{\iota, h}$  for different values of  $\iota$  and  $h$  with  $\lambda = \mu = 1$ . We  
 416 observe that the convergence rate appears to be linear when  $\iota$  is large, while it turns  
 417 out to be quadratic when  $\iota$  is close to zero, which is consistent with the theoretical  
 418 prediction in the estimate (24).

419 Next, we test both elements over a nonuniform mesh. The initial mesh is generated  
 420 by the function “initmesh” of the partial differential equation toolbox of MATLAB.  
 421 The initial mesh consists of 872 triangles and 469 vertices, and the maximum mesh  
 422 size is  $h = 1/16$ ; See Fig. 2b. In Tables 3, 4, 5 and 6, we report the convergence rate  
 423 of both elements in the energy norm when  $\lambda = \mu = 1$  and  $\lambda = 10, \mu = 1$ . It seems

**Table 5** The convergence rate of the second element over nonuniform mesh with  $\lambda = \mu = 1$ 

$\iota \backslash h$	1/16	1/32	1/64	1/128	1/256	1/512
1e0	2.50e-1	1.44e-1	8.06e-2	4.29e-2	2.20e-2	1.11e-02
Rate		0.80	0.84	0.91	0.96	0.98
1e-1	1.88e-1	1.08e-1	6.02e-2	3.20e-2	1.64e-2	8.30e-3
Rate		0.80	0.84	0.91	0.96	0.98
1e-2	3.14e-2	1.65e-2	9.04e-3	4.77e-3	2.44e-3	1.23e-3
Rate		0.92	0.87	0.92	0.97	0.99
1e-3	1.34e-2	3.79e-3	1.24e-3	5.11e-4	2.48e-4	1.24e-4
Rate		1.82	1.62	1.27	1.04	1.00
1e-4	1.31e-2	3.43e-3	8.85e-4	2.28e-4	6.06e-5	1.82e-5
Rate		1.93	1.96	1.96	1.91	1.74
1e-5	1.31e-2	3.43e-3	8.80e-4	2.23e-4	5.61e-5	1.41e-5
Rate		1.93	1.96	1.98	1.99	1.99

**Table 6** The convergence rate of the second element over nonuniform mesh with  $\lambda = 10$  and  $\mu = 1$ 

$\iota \backslash h$	1/16	1/32	1/64	1/128	1/256	1/512
1e0	2.47e-1	1.35e-1	7.41e-2	3.99e-2	2.09e-2	1.07e-2
Rate		0.87	0.86	0.89	0.93	0.97
1e-1	1.87e-1	1.02e-1	5.59e-2	3.00e-2	1.58e-2	8.07e-3
Rate		0.88	0.86	0.89	0.93	0.97
1e-2	3.19e-2	1.59e-2	8.53e-3	4.55e-3	2.37e-3	1.21e-3
Rate		1.01	0.90	0.90	0.94	0.97
1e-3	1.43e-2	3.92e-3	1.25e-3	5.04e-4	2.43e-4	1.23e-4
Rate		1.87	1.65	1.31	1.05	0.99
1e-4	1.41e-2	3.63e-3	9.32e-4	2.39e-4	6.34e-5	1.88e-5
Rate		1.96	1.96	1.96	1.92	1.75
1e-5	1.41e-2	3.63e-3	9.29e-4	2.35e-4	5.92e-5	1.49e-5
Rate		1.96	1.97	1.98	1.99	1.99

424 the convergence rate is the same with that over the uniform mesh. The first element is  
 425 slightly more accurate than the second one, in particular over the nonuniform mesh.

## 426 5 Conclusion

427 We prove a Korn-like inequality and its discrete analog for the strain gradient elastic  
 428 problem, which is crucial for the well-posedness of the underlying variational problems  
 429 as the Korn's inequality for the linearized elasticity. Guided by the discrete Korn's  
 430 inequality, we constructed two nonconforming elements that converge uniformly in  
 431 the microscopic parameter with optimal convergence rate. Numerical experiments

432 validate the theoretical results. The extension of the elements to three dimensional  
 433 problem and to high order would be very interesting and challenging. Applications  
 434 of these elements to realistic problem in strain gradient plasticity is another topic  
 435 deserves further pursuit. We leave all these issues in a forthcoming work.

436 **Acknowledgements** The work of Li was supported by Science Challenge Project No. TZ 2016003. The  
 437 work of Ming was partially supported by the National Natural Science Foundation of China for Disting-  
 438 guished Young Scholars 11425106, and National Natural Science Foundation of China Grants 91630313,  
 439 and by the support of CAS NCMIS. The work of Shi was partially supported by the National Natural  
 440 Science Foundation of China Grant 11371359. We are grateful to the anonymous referees for their valuable  
 441 suggestions.

## 442 References

- 443 1. Adams, R., Fournier, J.: Sobolev Spaces, 2nd edn. Academic, New York (2003)
- 444 2. Akarapu, S., Zbib, H.: Numerical analysis of plane cracks in strain-gradient elastic materials. *Int. J.*  
 445 *Fract.* **141**, 403–430 (2006)
- 446 3. Altan, S., Aifantis, E.: On the structure of the mode III crack-tip in gradient elasticity. *Scr. Metal.*  
 447 *Mater.* **26**, 319–324 (1992)
- 448 4. Amanatidou, E., Aravas, N.: Mixed finite element formulations of strain-gradient elasticity problems.  
 449 *Comput. Methods Appl. Mech. Eng.* **191**, 1723–1751 (2006)
- 450 5. Argyris, J., Fried, I., Scharpf, D.: The Tuba family of plate elements for the matrix displacement  
 451 method. *Aeronaut. J. R. Aeronaut. Soc.* **72**, 701–709 (1968)
- 452 6. Askes, H., Aifantis, E.: Numerical modeling of size effects with gradient elasticity-formulation, mesh-  
 453 less discretization and examples. *Int. J. Frac.* **117**, 347–358 (2002)
- 454 7. Bell, K.: A refined triangular plate bending element. *Int. J. Numer. Methods Eng.* **1**, 101–122 (1969)
- 455 8. Berger, A., Scott, R., Strang, G.: Approximate boundary conditions in the finite element method. *Symp.*  
 456 *Math.* **X**, 295–313 (1972)
- 457 9. Brenner, S.: Korn's inequalities for piecewise  $H^1$  vector fields. *Math. Comp.* **73**, 1067–1087 (2004)
- 458 10. Brenner, S., Neilan, M.: A  $C^0$  interior penalty method for a fourth order elliptic singular perturbation  
 459 problem. *SIAM J. Numer. Anal.* **49**, 869–892 (2011)
- 460 11. Ciarlet, P.: The Finite Element Method for Elliptic Problems. North-Holland, Amsterdam (1978)
- 461 12. Ciarlet, P., Raviart, P.A.: General Lagrange and Hermite interpolation in  $R^n$  with applications to finite  
 462 element methods. *Arch. Rational Mech. Anal.* **46**, 177–199 (1972)
- 463 13. Cosserat, E., Cosserat, F.: Theorie des corps deformables. Herman et fils, Paris (1909)
- 464 14. Exadaktylos, G., Aifantis, E.: Two and three dimensional crack problems in gradient elasticity. *J. Mech.*  
 465 *Behav. Mater.* **7**, 93–118 (1996)
- 466 15. Falk, R.: Nonconforming finite element methods for the equation of linear elasticity. *Math. Comput.*  
 467 **57**, 529–550 (1991)
- 468 16. Guzmán, J., Leykekhman, D., Neilan, M.: A family of non-conforming elements and the analysis of  
 469 Nitsche's method for a singularly perturbed fourth order problem. *Calcolo* **49**, 95–125 (2012)
- 470 17. Hansbo, P., Larson, M.: Discontinuous Galerkin methods for incompressible and nearly incompressibly  
 471 elasticity by Nitsche's method. *Comput. Methods Appl. Mech. Eng.* **191**, 1895–1908 (2002)
- 472 18. Korn, A.: Solution générale du problème d'équilibre dans la théorie de l'élasticité dans le cas où les  
 473 efforts sont donnés à la surface. *Ann. Fac. Sci. Toulouse Sci. Math. Sci. Phys. (2)* **10**, 165–269 (1908)
- 474 19. Korn, A.: Über einige ungleichungen, welche in der Theorie der elastischen und elektrischen  
 475 Schwingungen eine Rolle spielen. *Bull. Intern. Cracov. Akad. Umiejtnosci. (Classe Sci Math Nat)* pp  
 476 706–724 (1909)
- 477 20. Ma, Q., Clarke, D.: Size dependent hardness of silver single crystals. *J. Mater. Res.* **10**, 853–863 (1995)
- 478 21. Mardal, K., Winther, R.: An observation on Korn's inequality for nonconforming finite element meth-  
 479 ods. *Math. Comput.* **75**, 1–6 (2006)
- 480 22. Mardal, K., Tai, X., Winther, R.: A robust finite element method for Darcy–Stokes flow. *SIAM J.*  
 481 *Numer. Anal.* **40**, 1605–1631 (2002)
- 482 23. Mindlin, R.: Microstructure in linear elasticity. *Arch. Rational Mech. Anal.* **10**, 51–78 (1964)

- 483 24. Mindlin, R., Eshel, N.: On the first strain-gradient theories of linear elasticity. *Int. J. Solid Struct.* **4**,  
484 109–124 (1968)
- 485 25. Ming, P.B., Shi, Z.C.: Nonconforming rotated  $Q_1$  element for Reissner–Mindlin plate. *Math. Model*  
486 *Methods Appl. Sci.* **11**, 1311–1342 (2001)
- 487 26. Nilssen, T., Tai, X., Winther, R.: A robust nonconforming  $H^2$ -element. *Math. Comput.* **70**, 489–505  
488 (2001)
- 489 27. Papanastasiou, S.A., Zervos, A., Vardoulakis, I.: A three-dimensional  $C^1$  finite element for gradient  
490 elasticity. *Int. J. Numer. Eng.* **135**, 1396–1415 (2009)
- 491 28. Ru, C., Aifantis, E.: A simple approach to solve boundary-value problems in gradient elasticity. *Acta*  
492 *Mech.* **101**, 59–68 (1993)
- 493 29. Soh, A.K., Chen, W.: Finite element formulations of strain gradient theory for microstructures and the  
494  $C^{0-1}$  patch test. *Int. J. Numer. Methods Eng.* **61**, 433–454 (2004)
- 495 30. Wang, L., Wu, Y., Xie, X.: Uniformly stable rectangular elements for fourth order elliptic singular  
496 perturbation problems. *Numer. Methods Partial Differ. Equ.* **29**, 721–737 (2013)
- 497 31. Wei, Y.: A new finite element method for strain gradient theories and applications to fracture analyses.  
498 *Eur. J. Mech. A Solids* **25**, 897–913 (2006)
- 499 32. Zervos, A., Papanastasiou, P., Vardoulakis, I.: Modelling of localisation and scale effect in thick-walled  
500 cylinders with gradient elastoplasticity. *Int. J. Soilds Struct.* **38**, 5081–5095 (2001)
- 501 33. Zervos, A., Papanastasiou, S.A., Vardoulakis, I.: Two finite element discretizations for gradient elas-  
502 ticity. *J. Eng. Mech.* **135**, 203–213 (2009)

Uncorrected Proof